

Corresponding states correlation for the saturated vapor pressure of pure fluids

Kh. Mejbri, A. Bellagi*

U.R. Thermique et Thermodynamique des Procédés Industriels, E.N.I.M., Av. Ibn Jazzar, 5060 Monastir, Tunisia

Received 5 March 2005; received in revised form 22 June 2005; accepted 27 June 2005

Abstract

A new simple equation for the vapour-pressure of pure substances is proposed. It is a three-constant non linear correlation that reproduces with high accuracy the vapor–liquid equilibrium data, even at low reduced temperatures. Applied to 34 fluids with acentric factors varying in the range between -0.4 and $+0.4$, the model is shown to be very performant. The average relative deviation between the data and the estimated values is in the order of 0.16% , with a maximum at 0.3% . Based on this model an accurate three-parameter generalized vapor pressure correlation which needs P_c , T_c and ω as inputs is established.

© 2005 Elsevier B.V. All rights reserved.

Keywords: Vapour pressure; Pure fluids ; Corresponding-states correlation

1. Introduction

The variation of saturated vapor pressure with temperature is given by the exact Clausius–Clapeyron equation:

$$\frac{d \ln P_r}{d(1/T_r)} = - \frac{\Delta H_{\text{vap}}}{RT_c \Delta Z_{\text{vap}}} = -\psi \quad (1)$$

where $\Delta H_{\text{vap}} \equiv (H_v - H_l)$ is the molar enthalpy of evaporation, $\Delta Z_{\text{vap}} \equiv (Z_v - Z_l)$, the compressibility variation at phase change, T_c , the critical temperature. P_r and T_r are the reduced pressure and temperature. The integration of Eq. (1) requires the knowledge of the function $\psi(T_r)$ (i.e. the dependence of ψ on temperature) which can not be deduced from thermodynamic principles. Instead, it is usually resorted to empirical correlations of the integrated form of Eq. (1).

Relation (1) suggests that the logarithm of the reduced vapor pressure can be expressed as a function of τ , the inverse of the reduced temperature, ($\tau = 1/T_r$),

$$\ln P_r = f(\tau). \quad (2)$$

Numerous empirical vapor-pressure equations have been published, the best known are those of Clausius, Antoine,

Frost–Kalkwarf, Cox, Gomez–Thodos, Lee–Kesler, Wagner, Ambrose–Walton, Riedel [1,2] and Lemmon–Goodwin [3]. We propose in this paper a new simple model that accurately reproduces the vapor pressure behavior over a wide range of the liquid–vapor coexistence region. Based on this model a predictive three-parameter corresponding-states correlation is established.

2. Correlation

We consider the following five-parameter expression for $f(\tau)$

$$\ln P_r = \alpha_1 + \alpha_2 \tau + \alpha_3 \tau^{\alpha_4} + \alpha_5 \exp(-\tau). \quad (3)$$

Because of the critical point condition ($P_r = 1$ at $\tau = 1$), the number of its adjustable coefficients is reduced to four. The equation reads then

$$\ln P_r = \alpha_1(1 - \exp(1 - \tau)) + \alpha_2(\tau - \exp(1 - \tau)) + \alpha_3(\tau^{\alpha_4} - \exp(1 - \tau)). \quad (4)$$

By applying the statistical optimization procedure described in [4] and [5] it is found that the first term in this equation can be omitted, thus further reducing the number of

* Corresponding author.

E-mail address: A.Bellagi@enim.rnu.tn (A. Bellagi).

Nomenclature

a, b, c and d	coefficients in Eq. (20)
A, B, C, D	coefficients in Eq. (28)
f, f_0, f_1, g_0, g_1 and g_2	temperature functions
ΔH_{vap}	heat of vaporization
N	number of data points used in the fitting
P	pressure
R	gas constant
T	temperature
Z	compressibility factor

Greek letters

α_i	coefficients in Eqs. (3) and (4)
β_i	coefficients in Eq. (5)
γ_i	coefficients in Eqs. (23) and (24)
τ	inverse of the reduced temperature
ψ	dimensionless group in Eq. (1)
ω	acentric factor

Subscripts

b	normal boiling point
c	critical state
cal	calculated value
exp	experimental value
l	liquid phase
v	vapor phase
r	reduced

parameters to three, and hence

$$\ln P_r = \beta_1(\tau - \exp(1 - \tau)) + \beta_2(\tau^{\beta_3} - \exp(1 - \tau)). \quad (5)$$

It is this model that will be used in the following for the correlation of the vapor pressure of pure fluids. As can be noted, the critical point condition is still verified by this relation.

According to Eq. (5), $f(\tau)$ is a linear combination of the two terms $(\tau - e^{1-\tau})$ and $(\tau^{\beta_3} - e^{1-\tau})$. The first term is positive monotonic and quasi-linear for $\tau \geq 1$. It can be regarded as the major term in the equation and the second term as a minor correcting one, i.e.

$$(\tau - e^{1-\tau}) \gg |(\tau^{\beta_3} - e^{1-\tau})|. \quad (6)$$

It follows that for the correct reproduction of the overall shape of the $(\ln P_r - \tau)$ -curve (negative function with a negative slope),

- β_1 must be negative,

$$\beta_1 < 0 \quad (7)$$

- and β_3 must be less than one,

$$\beta_3 < 1 \quad (8)$$

to avoid the divergence of the term $(\tau^{\beta_3} - e^{1-\tau})$ for larger values of τ .

To ensure that model (5) has the mathematical flexibility to reproduce the right shape of the $(\ln P_r - \tau)$ -curve, in particular that it predicts the existence of an inflexion point, the first and the second derivative of ψ ,

$$\frac{d\psi}{dT_r} = \tau^2[\beta_2\beta_3(\beta_3 - 1)\tau^{\beta_3-2} - (\beta_1 + \beta_2)\exp(1 - \tau)], \quad (9)$$

$$\frac{d^2\psi}{dT_r^2} = \frac{\tau^3(\beta_1 + \beta_2)}{\exp(1 - \tau)} \left\{ \left[\frac{\beta_2\beta_3(\beta_3 - 1)\tau^{\beta_3-2}}{(\beta_1 + \beta_2)\exp(1 - \tau)} \right] \times (-\beta_3) - \tau + 2 \right\}. \quad (10)$$

must be equal to zero. From Eq. (9) we can deduce that the three β coefficients must be such

$$\frac{\tau_f^{\beta_3-2}}{\exp(1 - \tau_f)} = \frac{\beta_1 + \beta_2}{\beta_2\beta_3(\beta_3 - 1)} \quad (11)$$

where τ_f is the value of τ at the inflexion point. Since the left-hand side of this equation is positive, so is also the right-hand side,

$$\frac{\beta_1 + \beta_2}{\beta_2\beta_3(\beta_3 - 1)} > 0. \quad (12)$$

If this inflexion point is to correspond to a *minimum* in the $(\psi - T_r)$ -curve, the second derivative of ψ (10) must be positive; the following condition should further be fulfilled

$$(\beta_1 + \beta_2)(-\beta_3 - \tau_f + 2) > 0. \quad (13)$$

From Eqs. (7)–(13) it is deduced that

- if $(\beta_1 + \beta_2) > 0$, then

$$\beta_2 > 0; \quad \beta_2 > |\beta_1|; \quad \beta_3 < 0 \quad (14)$$

- and if $(\beta_1 + \beta_2) < 0$, then

$$|\beta_1| > \beta_2 > 0; \quad 2 - \tau_f < \beta_3 < 1 \quad (15)$$

and hence

$$\beta_3 \in [0.57, 1[$$

if the minimum in the $(\psi - T_r)$ -curve is to be found at some value of T_r between 0.7 and 1.

It is interesting to note that both conditions (14) and (15) cause β_1 and β_2 to have opposite signs,

$$\text{sgn}(\beta_1) = -\text{sgn}(\beta_2).$$

3. Database

The main characteristics of the considered fluids are summarized in Table 1. T_{min} in these tables stands for the lower

Table 1
Main characteristics of the considered fluids

Fluid	ω	T_c (K)	P_c (MPa)	N	T_{\min} (K)	T_b (K)
H ₂ O	0.3443	647.1	22.064	1500	270.65	373.15
N ₂	0.0372	126.247	3.3984	357	63.15	77.355
Ar	-0.00219	150.69	4.8653	236	83.80	87.302
CH ₄	0.01142	190.56	4.5992	51	90.69	111.67
C ₂ H ₄	0.0866	282.35	5.0418	46	103.99	169.379
C ₂ H ₆	0.0993	305.33	4.8718	46	111.85	184.552
C ₃ H ₆	0.1408	365.57	4.6646	46	126.56	225.259
C ₃ H ₈	0.15243	369.85	4.2477	43	131.31	231.063
C ₄ H ₁₀	0.2	425.16	3.7960	48	154.67	272.60
<i>i</i> -C ₄ H ₁₀	0.185	407.85	3.64	45	148.87	261.48
C ₅ H ₁₂	0.251	469.7	3.3665	61	173.47	309.21
C ₆ H ₁₄	0.297	507.82	3.0181	32	197.83	341.86
C ₇ H ₁₆	0.348	540.13	2.7270	33	222.55	371.53
CO	0.051	132.8	3.4935	34	68.13	81.632
CO ₂	0.22394	304.21	7.3843	41	216.48	239.823
NH ₃	0.25601	405.4	11.333	51	195.49	239.823
O ₂	0.0222	154.58	5.0426	51	54.361	90.188
F ₂	0.0449	144.414	5.1724	46	53.481	85.037
Kr	-0.0017	209.48	5.5100	20	115.77	119.78
Ne	-0.0387	44.4918	2.6786	21	24.56	27.104
Xe	0.0036	289.734	5.8400	27	161.36	165.03
NF ₃	0.126	234	4.4607	31	85.00	144.138
He	-0.382	5.1953	0.22746	22	2.177	4.23
D ₂	-0.175	38.34	1.6653	21	18.71	23.3097
H ₂	-0.214	33.19	1.315	40	13.96	20.39
R22 ^a	0.22082	369.295	4.990	48	135.73	232.34
R32 ^b	0.2769	351.26	5.782	54	136.34	221.50
R123 ^c	0.28192	456.83	3.6618	51	173.27	300.97
R124 ^d	0.2881	395.425	3.6243	26	150.00	261.19
R125 ^e	0.3061	339.33	3.6290	52	172.52	225.02
R134a ^f	0.32684	374.24	4.0593	52	169.85	247.08
R143a ^g	0.2615	345.86	3.7610	38	161.34	225.91
R152a ^h	0.27521	386.41	4.51675	48	154.56	249.13
C ₃ H ₆ O	0.304	508.10	4.7	11	178.2	329.65

$T_{\max} = T_c$ for all the considered fluids.

^a Monochlorodifluoromethane.

^b Difluoromethane.

^c 2,2-Dichloro-1,1,1-trifluoroethane.

^d 2-Chloro-1,1,1,2-tetrafluoroethane.

^e Pentafluoroethane.

^f 1,1,1,2-Tetrafluoroethane.

^g 1,1,1-Trifluoroethane.

^h 1,1-Difluoroethane.

limit of the temperature range investigated ; the upper limit is always the critical temperature T_c ; ω is the Pitzer acentric factor given by

$$\omega \equiv -1 - \log_{10}(P_r |_{T_r=0.7}), \quad (16)$$

N , the number of data points used for the determination of the adjustable parameters and T_b , the normal boiling temperature.

The vapor pressure data of water, argon and nitrogen are taken from reference [4] and those of acetone from [2]. The saturation properties of the rest of the fluids are taken from the *NIST* data bank [6].

4. Results and discussion

The saturation data are fitted with Eq. (5) using the FORTRAN version of ODRPACK [7], a fitting program based on the generalized least squares method. The significance of the adjustable three parameters β_i and the reliability of the whole correlation are checked using the Student and Fisher tests performed with the help of the Harwell library subroutines SA02 and SA03 [8] that we incorporated in the program.

The coefficients β_1 , β_2 and β_3 of model (5) are given in Table 2. Fig. 1 shows, as an illustration of the obtained results, the calculated vapor pressure curves for some of the considered fluids in comparison with the source data.

Table 2
Coefficients of model (5), $\langle \text{err} \rangle$ and percent errors err_{max} for the considered fluids

Fluid	β_1	β_2	β_3	$\langle \text{err} \rangle$	err_{max}
H ₂ O	-8.42427103	17.6878855	-0.467477372	0.30	2.48
N ₂	-5.86460860	11.3717828	-0.481031461	0.25	1.68
Ar	-5.58074373	11.3494987	-0.517884868	0.20	1.57
CH ₄	-5.52157708	10.7278920	-0.508083765	0.10	0.29
C ₂ H ₄	-6.52816808	13.8427584	-0.498394634	0.11	0.29
C ₂ H ₆	-6.52913380	13.8862104	-0.507187516	0.13	0.34
C ₃ H ₆	-7.08856217	15.5320335	-0.499162729	0.13	0.32
C ₃ H ₈	-7.12355886	15.2250575	-0.48659704	0.14	0.37
C ₄ H ₁₀	-7.60099458	16.5360612	-0.483849241	0.21	0.57
<i>i</i> -C ₄ H ₁₀	-7.63274376	17.1439208	-0.495323684	0.22	0.54
C ₅ H ₁₂	-8.23270729	18.7411026	-0.492014213	0.16	0.43
C ₆ H ₁₄	-8.70580376	19.1808993	-0.460785640	0.11	0.28
C ₇ H ₁₆	-9.40362956	21.7611373	-0.473588030	0.12	0.34
CO	-6.26120944	13.5042375	-0.514147519	0.18	0.64
CO ₂	-9.28701339	24.4108461	-0.517078992	0.07	0.21
NH ₃	-7.88513039	16.5178442	-0.464739920	0.16	0.40
O ₂	-5.71741316	11.3866949	-0.505907968	0.12	0.36
C ₃ H ₈ ^a	-7.21529330	16.8672426	-0.535532791	1.43	8.36
F ₂	-6.03674100	11.5202967	-0.456149755	0.11	0.72
Kr	-5.53399760	10.9677705	-0.509017150	0.06	0.16
Ne	-4.94257420	9.18457996	-0.527128185	0.07	0.13
Xe	-5.63921066	11.6032411	-0.522502377	0.10	0.25
NF ₃	-6.82733453	14.2586558	-0.482601178	0.16	0.45
R22	-7.93493424	17.6473483	-0.483737631	0.17	0.45
R32	-8.12085602	17.6069057	-0.479493292	0.14	0.46
R123	-8.74476364	20.1388857	-0.481297244	0.16	0.47
R124	-8.78802169	20.3550721	-0.484879639	0.15	0.45
R125	-9.00516287	20.9410002	-0.481295403	0.18	0.51
R134a	-9.08401095	20.6663189	-0.471560028	0.14	0.43
R143a	-8.19628188	18.2558993	-0.484913941	0.15	0.44
R152a	-8.29502777	18.3457812	-0.479826908	0.15	0.49
Acetone	-8.56196693	19.4099551	-0.49193080	0.31	1.18
He	-1.94633886	1.87905507	-1.009308470	0.21	0.66
H ₂	-2.90810127	2.91066037	-0.577067386	0.06	0.50
D ₂	-4.31046085	2.75237757	0.465408097	0.69	1.95

^a Fitted from melting point up.

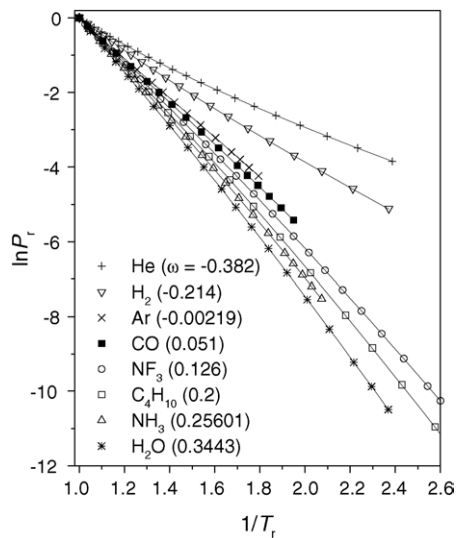


Fig. 1. Bibliographical and calculated (Eq. (5)) vapor pressures for some fluids in the $(\ln P_r, \tau)$ diagram.

To evaluate the accuracy of the proposed model, the following three criteria are used:

- the relative deviation, err , at point j :

$$\text{err} = 100 \left(\frac{P_{\text{cal}} - P_{\text{exp}}}{P_{\text{exp}}} \right)_j, \quad (17)$$

- the absolute average deviation in the entire temperature range, $\langle \text{err} \rangle$:

$$\langle \text{err} \rangle = \frac{100}{N} \sum_{j=1}^N \left| \frac{P_{\text{cal}} - P_{\text{exp}}}{P_{\text{exp}}} \right|_j, \quad (18)$$

- and the maximum absolute relative deviation, err_{max} , for a given fluid:

$$\text{err}_{\text{max}} = \text{Max} \left(100 \left| \frac{P_{\text{cal}} - P_{\text{exp}}}{P_{\text{exp}}} \right|_j \right). \quad (19)$$

The values of $\langle \text{err} \rangle$ and err_{max} are listed in the two last columns of Table 2. We notice that the average deviation is less than 0.3%, except for deuterium (0.7%), and that the

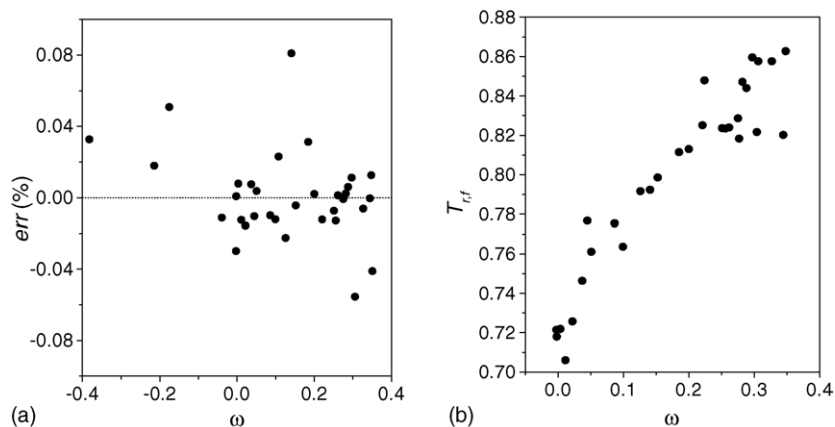


Fig. 2. (a) Percent error in the prediction of the normal boiling point temperature, T_b , of the considered substances; (b) location of the inflexion point on the $(\ln P_r, \tau)$ -curve for the different fluids.

maximum deviation, err_{max} , exceeds 0.8% only for water, nitrogen, argon and deuterium. It must be noted in the case of the three former fluids however that, unlike the smoothed data used for the others fluids, their saturation vapor pressures from reference [4] are raw experimental data that feature some scattering.

The normal boiling point T_b is an important characteristic of a substance and is a part of its identification in the CAS register. As Fig. 2a shows, it is predicted with high accuracy by model (5). The relative deviation between its reference and estimated values doesn't exceed 0.08% for all the considered fluids. It must be noted that correlation (5) has not been forced to reproduce the normal boiling point with a constraint in the fitting procedure.

A closer look at Table 2 reveals that, except for the quantum fluids He, H₂ and D₂, the three coefficients β_i verify solely condition (14). Furthermore, the value of β_2 is approximately twice that of $|\beta_1|$, and that of β_3 is roughly -0.5 . On Fig. 2b, the reduced temperature at which the inflexion point is exhibited, $T_{r,f}$, is shown vs. the acentric factor. As can be observed, the minimum in the $(\psi - T_r)$ -curve is located at T_r -values between 0.7 and 0.9 in accordance with the literature [2].

For He and D₂ none of conditions (14) and (15) is verified and no inflexion point is found. For hydrogen, condition (14) is fulfilled, but $(\beta_1 + \beta_2) \simeq 0$. From relation (11) it can be deduced that in this case τ_f must be very large (strictly speaking infinite) and hence outside the range of vapor–liquid region. In fact, the $(\psi - T_r)$ -curves for these

fluids, calculated with the *NIST* enthalpy and compressibility saturation data, do not show any minimum.

To compare our correlation with the four-parameter Wagner model [4]

$$\ln P_r = \frac{ax + bx^{1.5} + cx^{2.5} + dx^5}{T_r} \quad \text{with } x := 1 - T_r, \quad (20)$$

which is a very successful correlation recommended for the fitting of the vapor pressure data [1,2], we have determined its adjustable coefficients for five test fluids—water, nitrogen, argon, acetone and propane—using the same sets of data as for our model. The results are reported in Table 3. Fig. 3 shows the relative error in predicting the saturation pressures with the two correlations in comparison with the source data for water, nitrogen, argon and acetone. As can be noted, both models perform very well with $\langle err \rangle \leq 0.3\%$ for the four fluids. Furthermore they are comparable in the case of nitrogen ($\langle err \rangle = 0.3\%$), argon ($\langle err \rangle = 0.2\%$) and acetone ($\langle err \rangle = 0.3\%$). In the case of water the Wagner correlation is slightly better ($\langle err \rangle = 0.1\%$) than the proposed correlation ($\langle err \rangle = 0.3\%$).

Propane deserves a special treatment because of its very low triple point. When data from the entire liquid region - from the melting point up to the critical temperature - are used for the determination of the adjustable parameters of the two models, it is found that the Wagner correlation does

Table 3
Coefficients of the Wagner model and $\langle err \rangle$ for five test fluids

Fluid	a	b	c	d	$\langle err \rangle$
Water	-7.9316062	2.0838594	-2.5279984	-1.8404208	0.13
Nitrogen	-5.9399961	0.7478622	-0.1204184	-2.4853884	0.27
Argon	-5.9282312	1.2455884	-0.5947160	-1.4839174	0.17
Acetone ^a	-7.5368539	1.5752776	-1.9802628	-3.0595493	0.28
Propane	-6.8249981	1.7427737	-1.8478841	-1.8732377	0.10

^a 11 experimental data taken from Tables 7–3, ref. [2].

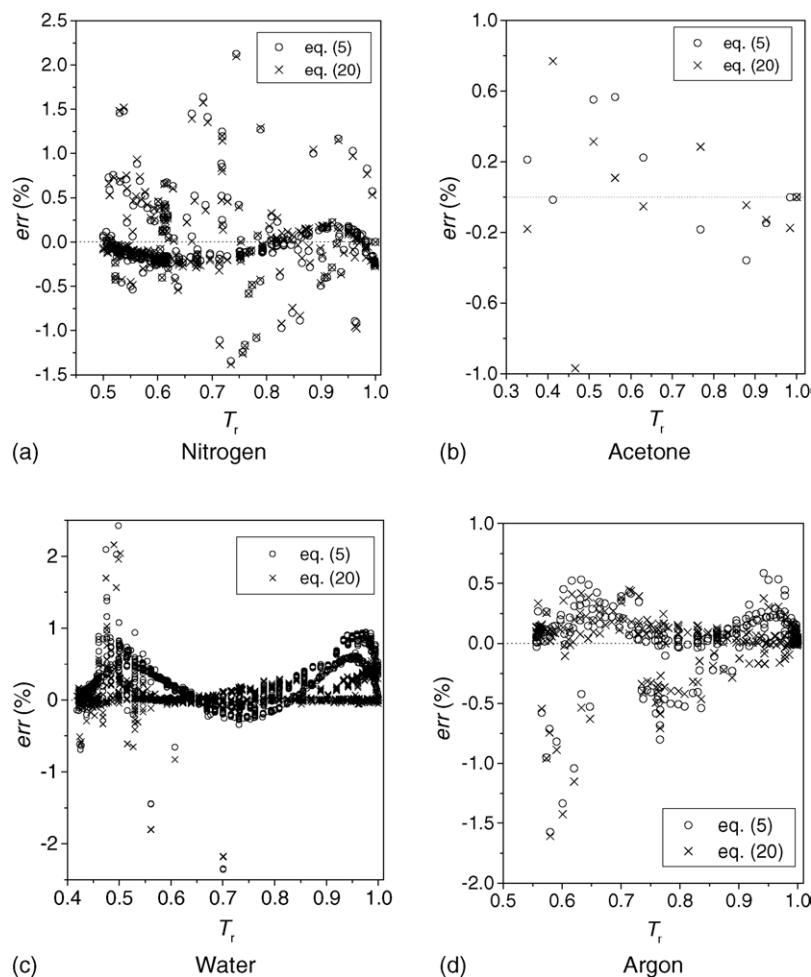


Fig. 3. Comparison of Eq. (5) to the Wagner model (20) in the cases of N_2 , C_3H_6O , H_2O and Ar.

better than model (5) with an average deviation $\langle \text{err} \rangle = 0.1\%$, against 1.4% for our model.

It can be concluded that, except for propane, both models are comparable in correlating the saturation vapor of the four test fluids. This comparison is particularly significant as the data used for the four fluids are experimental raw data that exhibit some scattering.

5. Model generalization

Correlation (5) is descriptive, fluid specific, and can not be used for prediction purposes. The large number of compounds of practical interest however—combined with the difficulty and high cost of the experimental determination of vapor pressures - renders prediction a valuable tool. Based on model (5) a predictive three-parameter generalized vapor pressure correlation will now be established.

5.1. Correlation

In Fig. 4a–c the coefficients β_1 , β_2 and β_3 of model (5) for the considered fluids are graphically represented vs. the

acentric factor ω . We note that β_1 and β_2 vary linearly with ω ,

$$\beta_1 = a + b\omega; \quad \beta_2 = c + d\omega$$

while β_3 is roughly constant

$$\beta_3 \simeq -0.5$$

Incorporating these observations in Eq. (5) leads to the generalized relation

$$\begin{aligned} \ln P_r &= (a + b\omega)(\tau - \exp(1 - \tau)) + (c + d\omega) \\ &\quad \times \left(\frac{1}{\sqrt{\tau}} - \exp(1 - \tau) \right) \\ &= \left[a(\tau - \exp(1 - \tau)) + c \left(\frac{1}{\sqrt{\tau}} - \exp(1 - \tau) \right) \right] \\ &\quad + \omega \left[b(\tau - \exp(1 - \tau)) + d \left(\frac{1}{\sqrt{\tau}} - \exp(1 - \tau) \right) \right] \end{aligned} \quad (21)$$

which shows that the reduced vapor pressure of the different pure fluids can be approximately expressed by a unique function of the inverse of the reduced temperature and the acentric factor. Furthermore, this function is linear in ω .

To gain more insight in the relation between $\ln P_r$ and ω , 60 isotherms are constructed for the reduced temperature range from 0.3 to 1, using vapor–liquid equilibrium data for all the pure substances considered in the present work. Fig. 4d shows some of them. Confirmation of the linear relationship between $\ln P_r$ and ω is found in every case, such that we can adopt the truncated form of the Pitzer expansion for the vapor pressure

$$\ln P_r = f_0(\tau) + \omega f_1(\tau). \quad (22)$$

For the temperature functions $f_0(\tau)$ and $f_1(\tau)$ we set the analytical expression of our model (Eq. (5)),

$$f_0(\tau) = \gamma_1(\tau - \exp(1 - \tau)) + \gamma_2(\tau^{\gamma_3} - \exp(1 - \tau)) \quad (23)$$

$$f_1(\tau) = \gamma_4(\tau - \exp(1 - \tau)) + \gamma_5(\tau^{\gamma_6} - \exp(1 - \tau)) \quad (24)$$

instead of the simplified expressions deduced from Eq. (21). This procedure greatly improves the accuracy of the resulting relation, mainly because β_3 (supposed to be equal to -0.5 in Eq. (21)) is not exactly constant.

The determination of the six adjustable coefficients γ_i is performed by fitting the set of Eqs. (22)–(24) to a vapor–liquid equilibrium data set of 1853 data points (roughly 50 points for each fluid) built out of the saturation data bank used in the first part of this paper.

5.2. Results and discussion

The values of the six universal coefficients γ_i are given in Table 4. Fig. 5a illustrates the evolution of the functions f_0 and f_1 with T_r . As shown in Fig. 5b, estimated values of the vapor pressure and source data are close together. Larger deviations are found only at very low reduced pressures. The overall absolute average deviation is 0.9%. The obtained corresponding-states correlation (22) reproduces therefore with a good accuracy the saturation pressure curves of pure fluids.

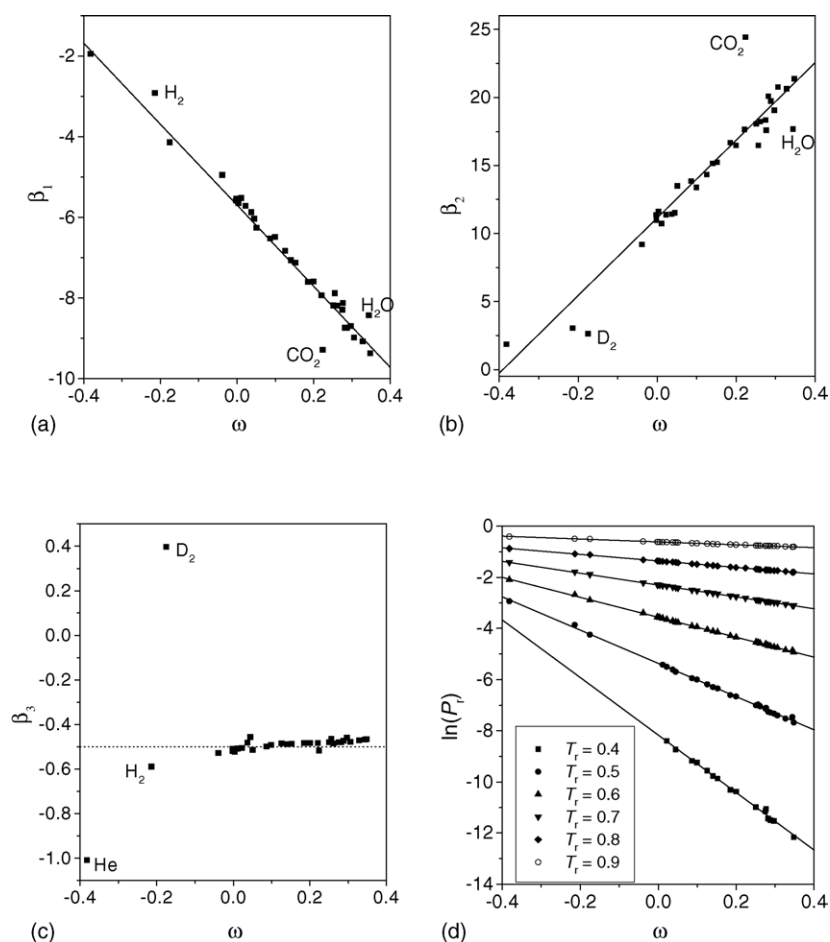


Fig. 4. (a) Parameter β_1 has a negative slope linear tendency with respect to ω ; (b) parameter β_2 is distributed around a positive slope straight line as function of ω ; (c) parameter β_3 takes values in the neighborhood of -0.5 , except for D_2 and He ; (d) reduced vapor pressures vs. ω for several isotherms.

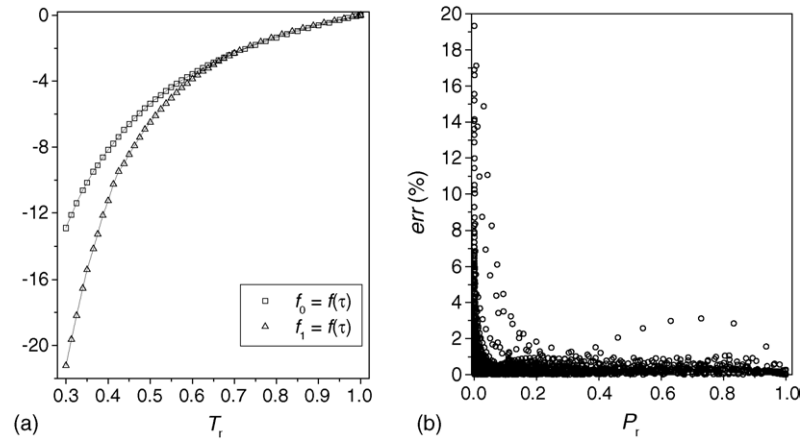


Fig. 5. (a) Tabulated and calculated (Eqs. (23) and (24)) values of the functions f_0 and f_1 representation with respect to T_r ; (b) Relative deviation $|err_j|$ between bibliographical and calculated (Eq. (22)) vapor pressures at various P_r .

Table 4
Coefficients of Eq. (22)

k	γ_k
1	-5.53357241
2	11.0210515
3	-0.51243147
4	-10.6722729
5	29.4364927
6	-0.44101891

To evaluate its predictive potential it will now be compared to four commonly used correlations:

- Lee–Kesler [1]

$$\ln(P_r) = 5.92714 - \frac{6.09648}{T_r} - 1.28862 \ln(T_r) + 0.169347T_r^6 + \omega \left[15.2518 - \frac{15.6875}{T_r} - 13.4721 \ln(T_r) + 0.43577T_r^6 \right] \quad (25)$$

- Ambrose–Walton [2]

$$\ln P_r = g_0 + \omega g_1 + \omega^2 g_2 \quad (26)$$

This correlation is a quadratic Pitzer expansion where the temperature functions g_0 , g_1 and g_2 have the same analytical expression as the Wagner model (20):

$$g_0 = \frac{-5.97616x + 1.29874x^{1.5} - 0.60394x^{2.5} - 1.06841x^5}{T_r}$$

$$g_1 = \frac{-5.03365x + 1.11505x^{1.5} - 5.41217x^{2.5} - 7.46628x^5}{T_r}$$

$$g_2 = \frac{-0.64771x + 2.41539x^{1.5} - 4.26979x^{2.5} + 3.25259x^5}{T_r} \quad (27)$$

- Lemmon–Goodwin [3]. This correlation has the same functional form as that of AMBROSE-WALTON, but is specific for alkanes as its coefficients are regressed to these fluids data for carbon number $n \leq 36$.
- Riedel [2]

$$\ln P_r = A - \frac{B}{T_r} + C \ln T_r + DT_r \quad (28)$$

with coefficients A , B , C and D estimated from the critical point coordinates, T_c and P_c , and the normal boiling point, T_b .

For the estimation of the vapor pressure with Eq. (22) the critical temperature and pressure (T_c , P_c) as well as the acentric factor, ω , are needed as inputs. If the latter is not known, it is recommended to estimate it from the normal boiling temperature T_b using the equation

$$\omega = \frac{0.013162987 - \ln P_c - f_0(\tau_b)}{f_1(\tau_b)} \quad (29)$$

with $\tau_b = T_c/T_b$ and P_c expressed in bar.

We show in Table 5 the detailed results of the comparison between the experimental vapor pressures and their corresponding values estimated with the five corresponding-sates correlations for nine fluids that are not considered in the construction of our equation: acetone, methanol, ethanol, n -C₁₂H₂₆, n -C₁₄H₂₈, n -C₁₆H₃₄, H₂S, SO₂ and HCl. For acetone, methanol, ethanol and n -C₁₂H₂₆ the percent deviations are also graphically represented vs. the reduced temperature in Fig. 6a–d. As can be observed, our correlation does better in the case of acetone on the whole temperature range, and at lower reduced temperatures, for most of the the other fluids.

The last row of Table 5 give the average error of the vapor pressure estimation for the nine test fluids. It turns out that the correlations of Riedel, Ambrose–Walton, Lee–Kesler and Eq. (22) are comparable, the two former being marginally better. If the comparison is made solely on the basis of the three alkanes of our test fluids, it is found that the Lemmon–

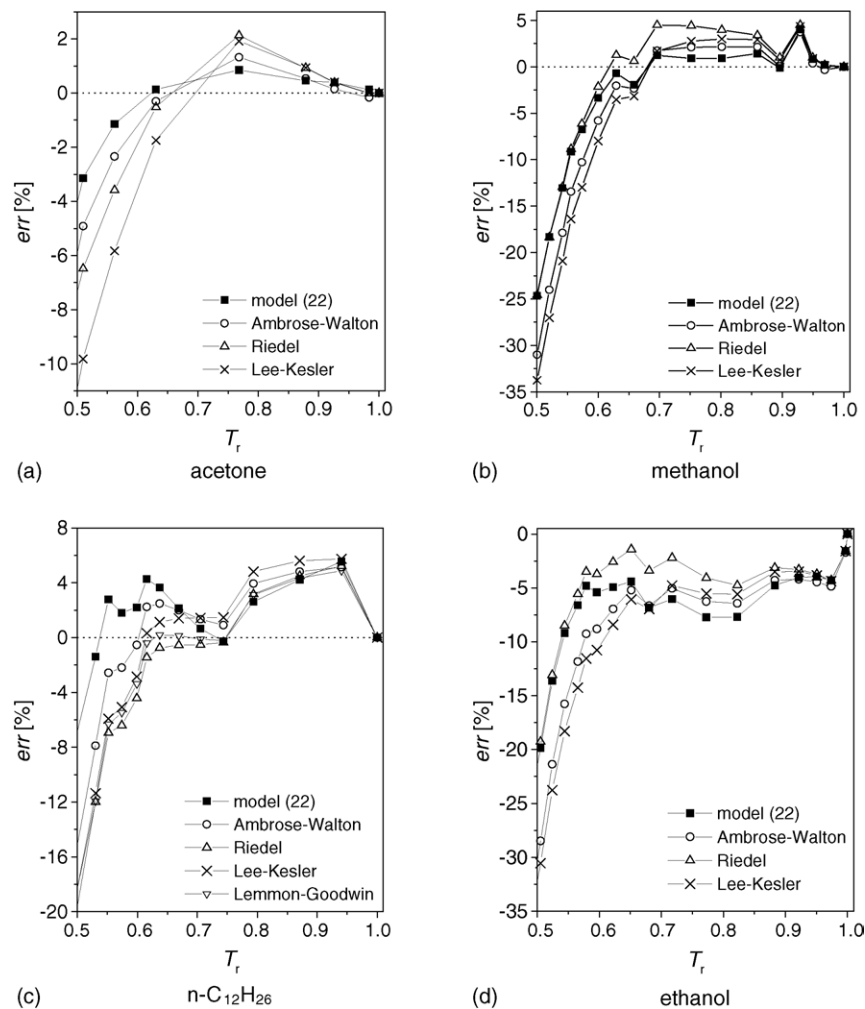


Fig. 6. Comparison of Eq. (22) to the Lee–Kesler, Ambrose–Walton, Riedel and Lemmon–Goodwin correlations. The percent error, *err*, is represented with respect to T_r .

Goodwin relation is the most accurate (2.3%), followed by the Ambrose–Walton equation (2.8%). This is mainly because these two relations were fit to the vapor pressure of this class of fluids and hence describe their behavior more accurately than ours (5.9%). In fact, higher alkanes were not used to establish our correlation, neither fluids with higher acen-

tric factor. When, on the other hand, the higher alkanes are discarded, Eq. (22) becomes slightly more accurate (5.2%) than the other relations, followed by the Riedel correlation (5.5%).

Finally, it is interesting to note that the vapor pressures of the two fictitious fluids of van der Waals and Redlich–Kwong

Table 5
Comparison of Eq. (22) to Ambrose–Walton, Riedel, Lee–Kesler and Lemmon–Goodwin correlations

Fluid	(err)					T range (K)	Ref.
	Eq.(20)	Ambrose–Walton	Riedel	Lee–Kesler	Lemmon–Goodwin		
Acetone	3.63	5.08	4.32	6.84		178–508	[2]
Methanol	8.13	10.8	8.77	12.2		229–513	[9]
Ethanol	7.73	10.2	5.72	10.8		242–516	[9]
H ₂ S	3.65	4.05	3.42	3.40		175–373	[9]
SO ₂	3.52	3.18	2.28	1.83		203–430	[9]
HCl	4.46	5.08	8.50	5.42		122–324	[9]
<i>n</i> -C ₁₂ H ₂₆	2.89	3.86	4.79	4.87	4.51	321–658	[9]
<i>n</i> -C ₁₄ H ₃₀	13.3	3.54	7.26	3.69	0.72	279–527	[9]
<i>n</i> -C ₁₆ H ₃₄	1.45	0.92	2.10	0.55	1.61	560–722	[10]
Average	5.4	5.2	5.2	5.5	2.28		

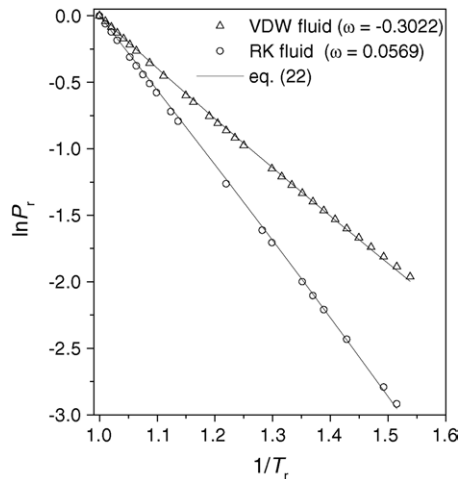


Fig. 7. Comparison of saturated vapor pressures of van der Waals and Redlich-Kwong fluids and their corresponding calculated (using model (22)) values in the $\ln P_r - \tau$ diagram.

[11] are accurately predicted by the universal correlation (22), as Fig. 7 shows, by just setting the values of the corresponding acentric factors ($\omega_{VDW} = -0.3022$; $\omega_{RK} = 0.0569$) in this equation.

6. Conclusion

A simple three-coefficient model is proposed for correlating the vapor pressure of pure fluids. Tested on about thirty substances with an acentric factor varying from -0.4 to $+0.4$, the correlation is found to be adequate and accurate over a wide range of vapor–liquid coexistence region. The overall absolute deviation averaged over all considered fluids is 0.16%. Based on this model, a general three-parameter

corresponding-states correlation is established needing the critical pressure and temperature as well as the Pitzer acentric factor as inputs. When compared to the commonly used correlations it seems to have a comparable to slightly better predictive potential by less mathematical complexity and fewer coefficients.

References

- [1] R.C. Reid, J.M. Prausnitz, B.E. Poling, *The Properties of Gases and Liquids*, fourth ed., McGraw-Hill, 1987, pp. 205–240.
- [2] B.E. Poling, J.M. Prausnitz, J.P. O'Connell, *The Properties of Gases and Liquids*, fifth ed., McGraw-Hill, 2001.
- [3] E.W. Lemmon, A.R. Goodwin, *J. Phys. Chem. Ref. Data* 29 (2000) 1–39.
- [4] W. Wagner, *Eine mathematisch statistische Methode zum Aufstellen thermodynamischer Gleichungen - gezeigt am Beispiel der Dampfdruckkurve reiner fluider Stoffe*, VDI-Verlag, Düsseldorf, Germany, 1974.
- [5] W. Wagner, *New vapor pressure measurements for Argon and Nitrogen and a new method for establishing rational vapor pressure equations*, *Cryogenics* 13 (1973) 470–482.
- [6] P.J. Linstrom, W.G. Mallard (Eds.), *NIST Chemistry WebBook*, NIST Standard Reference Database Number 69, July 2001. (<http://webbook.nist.gov>).
- [7] P.T. Boggs, R.H. Byrd, J.E. Rogers, R.B. Schnabel, *User's Guide for ODRPACK Version 2.01 Software for Weighted Orthogonal Distance Regression*, National Institute of Standards and Technology Interagency Report 4834, 1992.
- [8] Harwell Subroutine Library, HSL Archive packages.
- [9] R.H. Perry, C.H. Chilton, *Chemical Engineers' Handbook*, fifth ed., McGraw-Hill, 1973.
- [10] T.E. Parker, R.F. Sawyer, A.K. Oppenheim, *Thermodynamic Properties of Hydrocarbons*, Department of Mechanical Engineering and Applied Science Division, Lawrence Berkeley Laboratory, University of California, Berkeley, CA 94720, 1975.
- [11] J.W. Tester, M. Modell, *Thermodynamics and its Applications*, third ed., Prentice Hall, 1997.